Thermal characterization of defects in aircraft structures via spatially controlled heat application

K. Elliott Cramer
and
William P. Winfree

NASA - Langley Research Center
3 E. Taylor St. - MS 231
Hampton, VA 23681-0001

ABSTRACT

Recent advances in thermal imaging technology have spawned a number of new thermal NDE techniques that provide quantitative information about flaws in aircraft structures. Thermography has a number of advantages as an inspection technique. It is a totally noncontacting, nondestructive, imaging technology capable of inspecting a large area in a matter of a few seconds. The development of fast, inexpensive image processors have aided in the attractiveness of thermography as an NDE technique. These image processors have increased the signal to noise ratio of thermography and facilitated significant advances in post-processing. The resulting digital images enable archival records for comparison with later inspections thus providing a means of monitoring the evolution of damage in a particular structure.

The National Aeronautics and Space Administration's Langley Research Center has developed a thermal NDE technique designed to image a number of potential flaws in aircraft structures. The technique involves injecting a small, spatially controlled heat flux into the outer surface of an aircraft. Images of fatigue cracking, bond integrity and material loss due to corrosion are generated from measurements of the induced surface temperature variations. This paper will present a discussion of the development of the thermal imaging system as well as the techniques used to analyze the resulting thermal images. Spatial tailoring of the heat coupled with the analysis techniques represent a significant improvement in the delectability of flaws over conventional thermal imaging.

Results of laboratory experiments on fabricated crack, disbond and material loss samples will be presented to demonstrate the capabilities of the technique. An integral part of the development of this technology is the use of analytic and computational modeling. The experimental results will be compared with these models to demonstrate the utility of such an approach.

Keywords: thermography, infrared imaging, corrosion, aging aircraft, nondestructive inspection

2. INTRODUCTION

The use of spatially controlled heat application has been shown to be beneficial for the detection of a number of types of flaws in both single layer and laminated structures. A fixed linear heat source has been used to detect such flaws as fatigue cracks[1]. Additionally, Maldague[2] described a system where a sample moving at a constant velocity passes a fixed linear heat source and is observed by an infrared imager. This technique has been shown to be effective in the detection of disbonding in laminated samples. This technique has certain advantages over conventional time dependent thermal imaging where the heat source, imager and sample are fixed, but the heating and inspection times are varied. Presented here are results from a system where heat is injected into a stationary sample by a linear heat source moving at a constant velocity. Images of the temperature variations induced in the sample are made with an infrared imager following, at the same velocity as the heat source, but separated by a fixed distance. One of the advantages of this type of system is the inspection speeds possible. This paper will present results of laboratory experiments on fabricated samples, representative of aircraft structures, as well as on actual aircraft structures that demonstrate the potential capabilities and advantages for this technique. The theoretical basis for this technique will also be presented.

3. EXPERIMENTAL TECHNIQUE

Figure 1 shows a block diagram of the thermal inspection system that has been developed. The thermal images are produced with a commercial infrared (IR) radiometer which uses a mechanically scanned HgCdTe (Mercury - Cadmium - Telluride) detector cooled to near liquid nitrogen temperatures by an closed cycle electric microcooler. The radiometer's minimum detectable temperature difference, cited by the manufacturer, is less than 0.1°C when operating the detector in the 8 to 12 micrometer range. The imaging radiometer produces images at the rate of 30 per second (video frame rate) in an RS170 format compatible with standard video equipment. External optics, consisting of a 0.5x wide-angle lens, using four germanium optical elements, was used to increase the system field-of-view by a factor of 2.

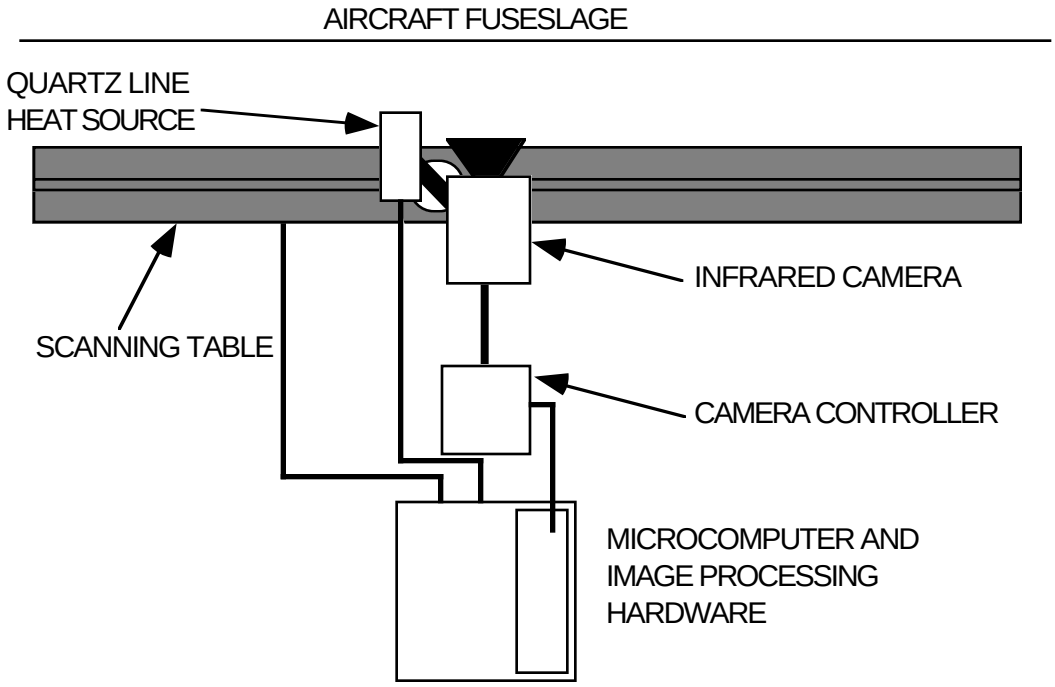

Figure 1. Block diagram showing infrared imaging system components.

Measurements are made by applying an approximate line of heat to the sample surface using a quartz lamp with an elliptical reflector behind the quartz tube to focus the energy into a line. Both the heat source and the IR imager are attached to a commercially available linear scanning bridge. To facilitate quantitative time based analysis, synchronization between the infrared imager, the heat source and the scanning table is required. This synchronization is achieved by controlling the application of heat from the 1000 watt quartz lamp with the host computer for the image processor. Currently, the scanning table is controlled by a separate computer system and synchronization is achieved by starting the scan a fixed time before the start of data collection. Scanning speeds can be varied by the digital controls to provide any rate up to 30.5 cm/sec. In the future, the scanning table control will be integrated into the host computer for the image processor. For all cases presented in this paper the maximum surface temperature change of the sample above ambient never exceeded 10°C.

The signal from the radiometer is digitized and stored at video frame rates in a commercially available real-time image processor with a personal computer as a host. The image processor has eight megabytes of image memory available for storage making it possible to acquire 16 images, each of which contains 512 x 512 16-bit pixels. The image processor can also subsample the incoming video signal producing 256 images of 128 x 128 16-bit pixels each, and is capable of real-time averaging on the incoming video signal to increase signal to noise. Once the video signal is digitized the resulting images are transferred to the host

computer for archival and analysis. The computer is also configured with an input-output card which permits acquisition and production of analog and digital signals under program control.

If the surface being imaged has an emissivity of 1, then the resulting images are directly proportional to the surface temperature of the object. If the emissivity is less than 1 (typical bare aircraft aluminum has an emissivity of less than 0.1) then measurements made by the imager are a combination of the surface temperature of the object and reflections of background radiation sources. Therefore for low emissivity objects it is necessary to enhance the emissivity by the addition of a coating to the surface. Aircraft paint is typically a good emissivity coating, therefore if the aluminum is painted, regardless of color, no additional surface coating is necessary. Samples, which are normally unpainted, require the addition of an emissivity enhancement. For the results presented here, the samples are treated with a water washable, nontoxic paint to enhance the emissivity.

4. DATA ANALYSIS AND THEORY

The temperature distribution in a semi-infinite media with an infinitely long line source moving along the surface is given by[3]

$$T(x,z,t) = \frac{q}{\pi K} e^{-v(x-vt)/2\kappa} K_0[\frac{v((x-vt)^2+z^2)^{1/2}}{2\kappa}]$$

where v is the velocity of the moving line source, K and κ are the thermal conductivity and diffusivity respectively and q is the rate of heat emitted by the line source per unit length. K_0 is the modified Bessel function of the second kind of order zero. From this expression, temperature at the heated surface of a layer of thickness L is found to be

$$T(x,z,t) = \frac{q}{\pi K} e^{-v(x-vt)/2\kappa} (K_0[\frac{v|x-vt|}{2\kappa}] + 2\sum_{n=1}^{\infty} K_0[\frac{v((x-vt)^2+(2nL)^2)^{1/2}}{2\kappa}])$$

.

In the frame of reference moving with the heat source and centered on the line source, the temperature at the surface is given by

$$T(x,z,t) = \frac{q}{\pi K} e^{-vx/2\kappa} (K_0[\frac{v|x|}{2\kappa}] + 2\sum_{n=1}^{\infty} K_0[\frac{v(x^2+(2nL)^2)^{1/2}}{2\kappa}])$$

.

At a distance behind the heat source greater than $L^{3/2}$ for $Lv/\kappa < 25$, the temperature becomes a constant given by $q/(Lv\rho c)$.

For a thin layer of high diffusivity material, the temperature following the application of heat rapidly reaches a constant value which is inversely proportional to the thickness of the layer and as such gives a measurement of thickness of the layer. Therefore this temperature is a measurement of thickness of the layer. This condition lasts for as long as the approximation of the a infinite length line source on a sheet is adequate. Inplane heat flow due to effects such as the finite duration of the heating, variations in thickness of layer, finite size of the heating source will result in subsequent variations in the temperature. However for the window of time for which this does not occur, the temperature at a fixed point behind the source gives a good map of the thickness of the layer. For a bonded layer, the presence of a disbond will act as a change in the effective thickness of the material, giving a similar effect.

The imaging camera is moving with the heat source, enabling the acquisition of data at fixed distance from the source. To analyze the results a single image is reconstructed from the entire data set acquired at a single distance away from the heat source. The same column of data from each image in the time history recorded by the image processor is reassembled to form a reduced image. These resulting images are

typically 128 pixels high and 256 pixels wide (assuming that the data was collected in the 128 x 128 image mode of the image processor and all available memory was used). All of the data presented in the remainder of the paper was analyzed in this manner.

5. EXPERIMENTAL RESULTS

To initially investigate the capabilities of the thermal inspection system, a laboratory sample was constructed consisting of a single sheet of 2024-T3 aluminum approximately 15.25 cm wide, 76.2 cm long and 1.27 mm. thick. A material loss region 7.62 cm. wide and the full length of the sample was created by removing the aluminum down to a thickness of 1.0 mm. Figure 2 shows a schematic of the sample and the results of scanning at a rate of approximately 5.0 cm per second.

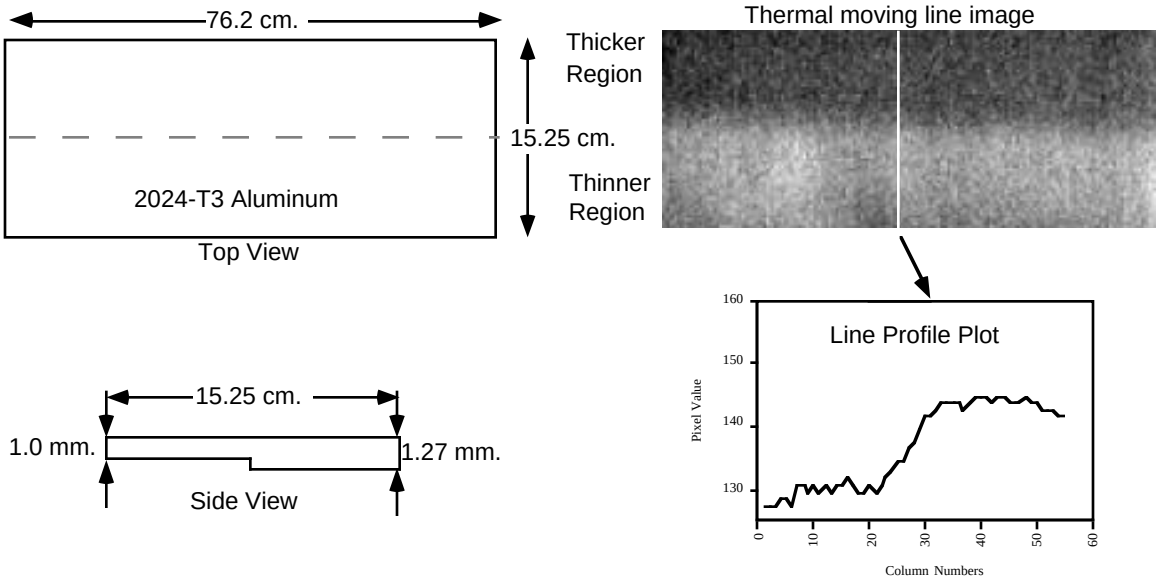

Figure 2. Schematic of two thickness aluminum sample and thermal line scan results which indicate the ability of the technique to discriminate material thickness.

To investigate the capabilities of the technique further, several lap joint type samples were fabricated. All were fabricated out of 2024-T3 aluminum sheets of thickness 1.0 mm. Each lap region is 7.62 cm. in width and is bonded together with a standard two part epoxy. A general schematic of the samples is shown in figure 3.

The samples have dimensions as listed in the following table.

Sample Number	Width	Height
Sample A	61 cm.	114.3 cm.
Sample B	45.7 cm.	83.8 cm.
Sample C	55.9 cm.	53.3 cm.

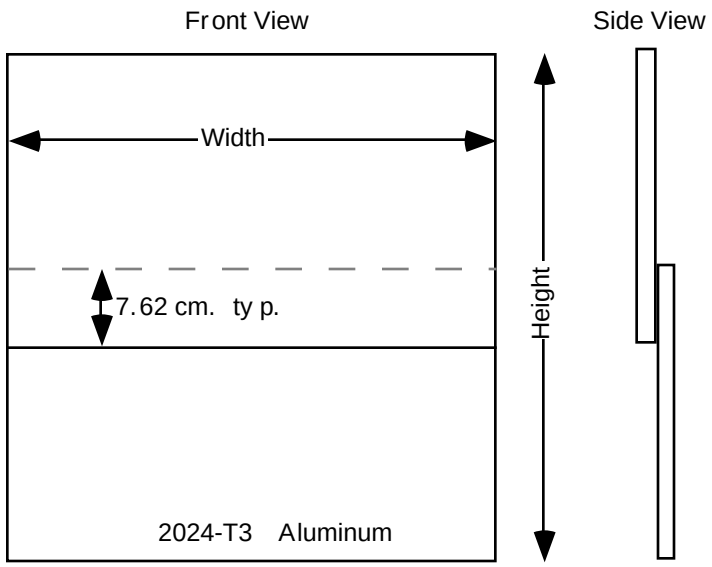

Figure 3. Schematic of typical lap type joint samples.

Sample A contains 3 disbonds fabricated into the lap joint region. The disbonds are 1.27, 2.54 and 3.81 cm. in width, are distributed uniformly across the entire width of the panel and extend across the total width of the lap joint region. The results for Sample A are shown in figure 4a. All three disbonds can be distinguished in the resulting image. Likewise some additional, unintentional disbonding can be observed near the smallest disbond. This additional disbonding has been confirmed using conventional thermography[4] as shown in figure 4b. These results also show the improved inspection rate compared to conventional quartz lamp thermography. The data was acquired with the moving line source in approximately 12 seconds, while conventional quartz lamp thermography would require approximately 72 seconds for comparable results. The data storage and analysis currently requires the same time for either technique. But results indicate that the analysis time could be significantly reduced for the moving line technique by utilizing the image processor's capabilities to do real-time integer processing on the data.

Sample B contains an imbedded region of material loss centered in the lap joint of the sample. This region was produced by removing approximately 25% of the thickness of the upper aluminum skin in a 2.54 cm. square region before the lap joint was bonded. To avoid filling the material loss region with epoxy during the bonding process a small piece of mylar (just larger than the material loss region) was bonded over the material loss region and allowed to cure before final bonding of the panel. Figure 5 shows the results of applying the moving line technique to this sample. In addition to the material loss region, a triangular region of disbonding is observable in the corner of the lap joint. This disbonding has been confirmed both by conventional thermography and by visual inspection of the sample.

Sample C contained both a disbond and a material loss region. The material loss region was again created by removing a small portion of the total thickness of the material. Approximately 0.2 mm. of aluminum was removed across a 2.54 cm. wide 5.0 cm long area. Next a brass shim of the same thickness and dimensions as the material loss region was inserted in that region. A second brass shim was placed approximately 15.25 cm. away from the material loss region and the sample was bonded to create a lap joint. After the epoxy had cured sufficiently, the brass shims were removed to form a disbond region and a material loss region in the same joint. Figure 6 shows the inspection results by the moving line technique. Figure 6 also shows a single line of data in which it is possible to see the difference in the amplitude of the thermal signal between the material loss region and the disbond region.

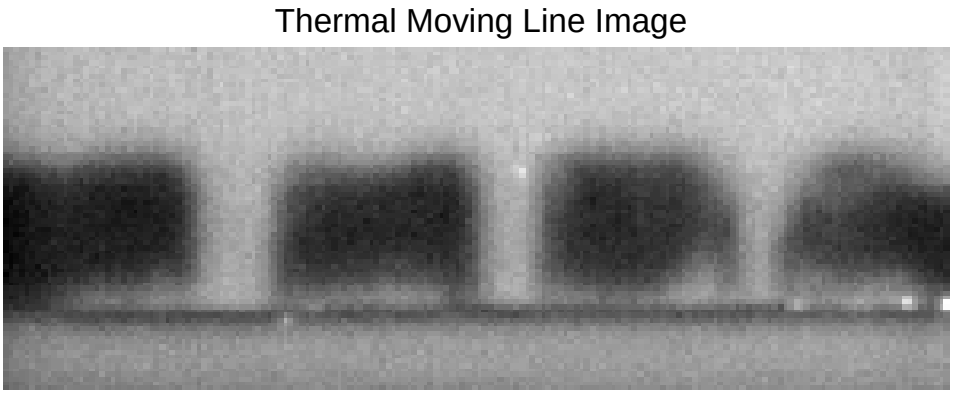

Figure 4. Comparison of moving line source technique (a) with conventional quartz lamp thermography on a lap joint sample with 3 fabricated disbonds.

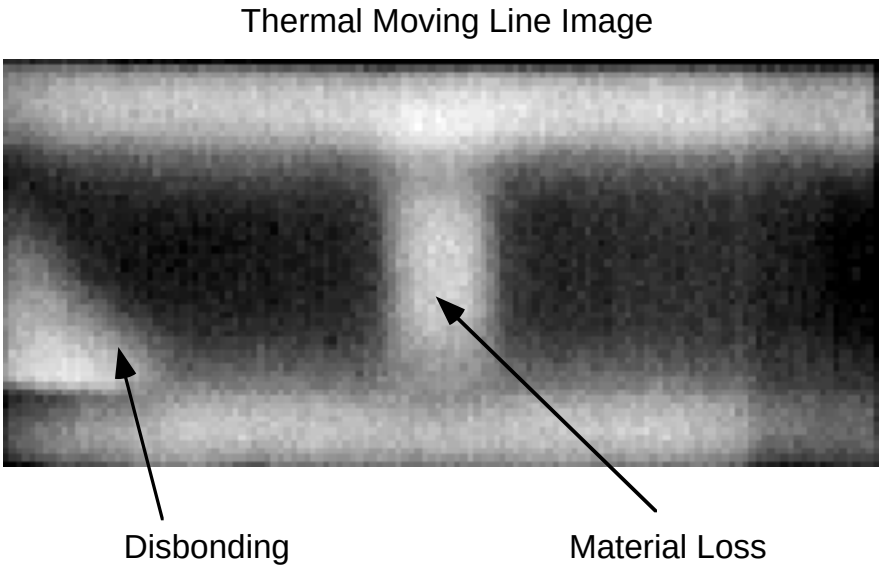

Figure 5. Results for Sample B with material loss and unintentional disbonding.

Finally, the technique was applied to a actual aircraft section. The sample was cut from a commercial aircraft which had been retired from service. The sample is 101.6 cm in width and 96.5 cm. in height. It consists of two 2024-T3 aluminum skins. The upper skin has a thickness of 21.6 mm. and the lower skin has a thickness of 16 mm. The skins are joined in a lap type joint were no bonding material was used but the joint was fastened by 3 rows of rivets. Since previous inspections of this sample indicated that there was no corrosion present in the lap joint, a 7.6 cm. square region adjacent to the lap joint was electrochemically corroded to produce a material loss of approximately 15%. Figure 7 shows the results for this sample. As can be seen a clear distinction can be made between the thicker upper skin, the thinner lower skin and the material loss region. Additionally, it is observable in the results that there is no bonding material in the lap joint, since the amplitude of the thermal signal over the lap joint is the same a in the upper skin.

6. SUMMARY AND FUTURE DIRECTIONS

A noncontacting thermal NDE technique has been developed which employs a moving line heat source and is capable of imaging defects in thin aluminum structures such as aircraft lap joints. This technique has been shown to effectively detect both disbonding and corrosion in thin aluminum laboratory samples as well as actual aircraft fuselage sections. Further, this technique has demonstrated the potential for discriminating between disbonding and corrosion. The technique is approximately 6 times faster than conventional quartz lamp thermography for thin structures. Additionally, the moving line source has the advantage that it is well suited to the inspection of long straight regions such as aircraft lap joints. Therefore, as longer and longer regions are inspected the speed advantages of this technique will continue to out weigh conventional thermography.

In the future additional analysis methods which take advantage of the use the entire thermal image that is produced by the radiometer should significantly improve the results and allow for quantitative analysis of the material loss. One such analysis method could involve reconstructing a series of images from the data acquired, each image at different distance from the heat source. These images could then be treated as a time series and variations in the heat propagation rates could be explored by such analysis methods as time derivatives. Further, for this technique to be applied in a practical manner additional work will be done on field implementation. This could potentially be accomplished by a linear robotic scanner which could efficiently transport the heat source and imager over large areas of and aircraft.

7. REFERENCES

1. K.E. Cramer, W.P. Winfree, P.A. Howell, H.I. Syed, K.A. Renouard, “Thermographic Imaging of Cracks in Thin Metal Sheets,” *Proceedings SPIE - Thermosense XIV*, Vol. 1682, pp. 162-170, April 1992.

2. X.P.V. Maldague, *Nondestructive Evaluation Of Materials By Infrared Thermography*, pp. 45-60, 83-93, Springer-Verlag, London, 1993.

3. H.S. Carslaw, J.C. Jaeger, *Conduction of Heat in Solids*, pp. 266-267, Clarendon Press, Oxford, 1959.

4. K.E. Cramer, P.A. Howell, H.I. Syed, “Quantitative Thermal Imaging of Aircraft Structures,” *Proceedings SPIE - Thermosense XVII*, Vol. 2473, pp. 226-232, April 1995.

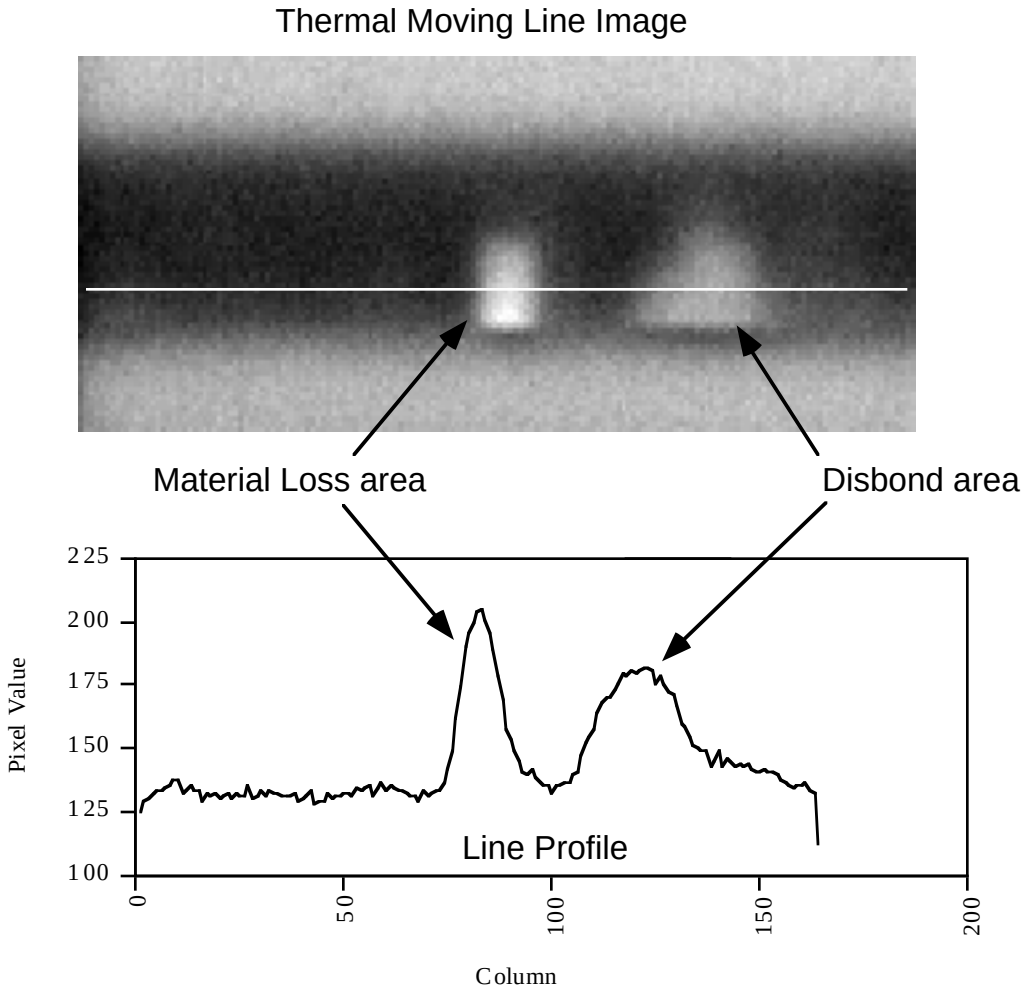

Figure 6. Results for Sample C with both disbonding and material loss. The line profile show the ability of the technique to distinguish the difference between the defect types.

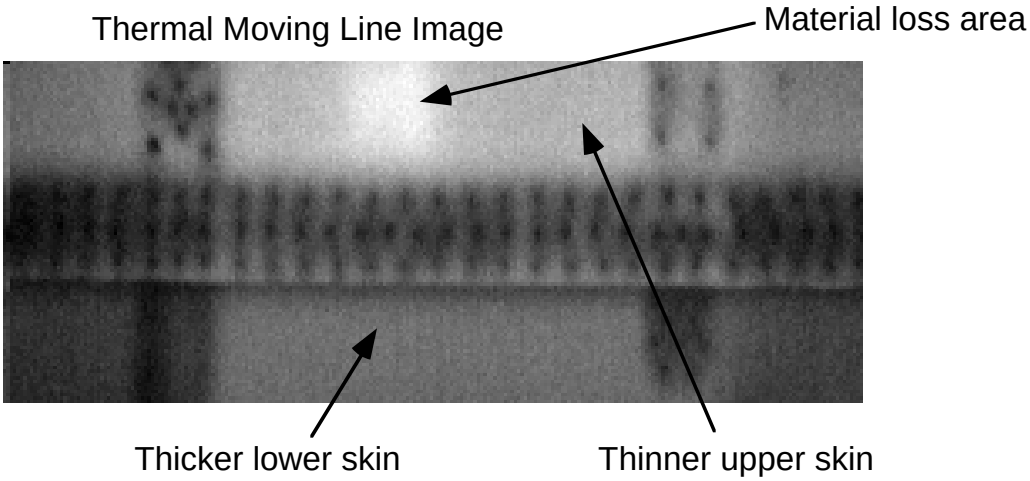

Figure 7. Results for actual aircraft sample with both no bonding in lap joint and material loss in skin immediately above joint. Differences in skin thickness can also be observed.